VILNIUS TECH
Vilnius Gediminas Technical University

Mokslas – Lietuvos ateitis / Science – Future of Lithuania
ISSN 2029-2341 / eISSN 2029-2252
2021 Volume 13, Article ID: mla.2021.12807, 1–6
https://doi.org/10.3846/mla.2021.12807

Civil engineering
Statybos inžinerija

DETERMINATION AND MODELLING OF BOND PROPERTIES OF SYNTHETIC MACRO-FIBRES IN CONCRETE

Mantas GARNEVIČIUS *, Linas PLIOPLYS, Viktor GRIBNIAK

Vilnius Gediminas Technical University, Vilnius, Lithuania

Received 27 May 2020; accepted 10 December 2020

Abstract. Bond behaviour of a synthetic macro-fibre in concrete is the object of this research. The bond strength and stiffness are the parameters characterising the bonding mechanism that determines the efficiency of the reinforcing material. However, there is no general methodology developed to evaluate fibre efficiency. There also exists neither a straightforward procedure to estimate the bond quality of a synthetic macro-fibre nor a reliable numerical model to simulate the bond behaviour of such fibres. In this work, the bond mechanisms of 40 mm long synthetic macro-fibres are investigated using pull-out tests: 16 concrete cubes were made for that purpose. One type of synthetic macro-fibre available at the market is considered. In each test sample, three fibres were inserted perpendicular to the top and two side surfaces; two bonding lengths (10 mm and 20 mm) were used. A gripping system was developed to protect the fibres from local damage. A physically non-linear finite element model of the pull-out sample was developed. A bond model was proposed to simulate deformation behaviour of the fibres.

Keywords: synthetic fibres, pull out, test, bond behaviour, numerical modelling.

Introduction

The RILEM recommendations TC 162 TDF (Vandewalle, 2000) considers fibre-reinforced concrete (FRC) as ordinary concrete with modified material properties. This approach is acceptable for design, but it does not allow to estimate the fibre interaction mechanisms or to define causes of alteration of mechanical properties of FRC. Variety of shapes, geometry and materials applied for the manufacturing of fibres complicates the issue. Recent publications (Sivakumar & Santhanam, 2007) demonstrated that synthetic fibres could be efficiently used in combination with steel fibres. However, the bond-behaviour of polymeric fibres was not investigated appropriately. Fibre length, concrete strength, the fibre content in concrete, fibre surface shape, the density of the concrete, and maximal size of the aggregates influence the bond performance (Babafemi & Boshoff, 2017; Alberti et al., 2016; Del Prete et al., 2019). It is difficult to determine which of these characteristics or combination of them is optimal for providing the most effective bond properties. The interaction (bond) mechanism of synthetic macro-fibres and concrete is the object of this research. This mechanism is responsible for the residual strength of FRC – the essential property describing the efficiency of the structural application of the fibres. The bond strength and the corresponding deformation modulus define the interaction mechanism. There is no universal methodology for evaluating these parameters. The adequacy of the determination of the bond properties is essential for the development of meso-scale numerical models of FRC (Oesch et al., 2018; Bitencourt et al., 2019). Figure 1 shows an example of the meso-model.

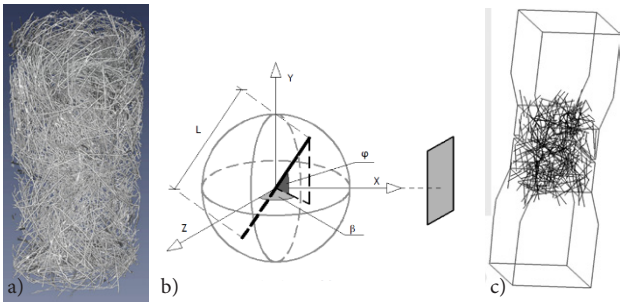

Figure 1. The modelling structure: a) experimental view of fibre reinforced concrete (Oesch et al., 2018); b) single fibre model; c) meso-model of FRC (Bitencourt et al., 2019)

*Corresponding author. E-mail: *garnevicius@vgtu.lt*

In this study, a pull-out test of a single fibre is applied to investigate the mechanical performance of the bond. The load-deformation diagram is the test outcome. One type of synthetic macro-fibre available at the market is considered. This study also aims to develop a numerical model enabling to predict deformation behaviour of synthetic macro-fibre pulled-out from the concrete.

1. Experimental program

One type of synthetic macro-fibre available at the market is considered (Figure 2a). A pull-out test of a single fibre is applied to investigate the mechanical performance of the bond. The fibres were pulled-out from 100 mm cubes. Two bonding lengths (10 mm and 20 mm) were used. Eight cubes were produced for each embedment length. Three fibres (one on the top and two on the opposite sides) were inserted in each cube (Figure 2b). The fibres were marked to assure a correct position, as shown in Figures 2a and 2b. The "side" fibres were positioned and fixed using expanded polystyrene (Figure 2c), while the "top" fibre in the specimen was placed manually. All samples were made in one batch. Proportions of 1 m^3 of concrete are following: 300 kg of cement CEM I 42.5 R, 165 l of water, 100 kg of limestone powder, 787 kg of 0/4 mm sand, and 988 kg of 4/16 mm crushed aggregates; 0.75% (by the cement weight) of the superplasticizer *Mapei Dynamon XTend*. Compressive strength of the 100 mm concrete cubes at 28 and the final testing (153) day was equal to 39.14 MPa and 46.16 MPa, respectively.

After the curing, the actual length of the outer (unbonded) part of fibre was measured. A plastic sleeve was used for protecting the unbonded part, as shown in Figure 2d; the fibre was fixed using steel clamps (Figure 2e) designed for preventing localization of stresses induced by the gripping system.

The tests were carried out using a 70 kN capacity electromechanical machine. The deformation-control path with the 0.8 mm/min velocity was applied. The load was fixed using a load-cell with 2.0 kN capacity. Linear variable differential transformers (LVDT) were used for monitoring vertical displacements of the grips, as shown in Figure 2f. Additional LVDT was used for monitoring vertical movements of the cube. All devices (LVDT and the load-cell) were connected to a personal computer through signal processing equipment ALMEMO 2890-9. The readings were taken every second. Table 1 summarises the test results.

Three failure types were identified: (I) extraction of fibre from the concrete (nominal outcome); (II) failure

Table 1. Summary of the pull-out tests results

Notation*	$\mathbf{P}_{max}$, N	$u_{\mathbf{p}}$, mm	δ, Nmm	u_{δ}, mm
1.1-1	176	4.90	938.3	10
1.1-2	198	4.86	1039.5	10
1.3-1	198	4.48	1175.3	10
1.3-2	224	4.76	330.8	5.55
1.4-1	213	5.02	1153.8	10
1.4-2	190	2.61	1080.2	10
2.1-1	197	5.79	656.6	7.21
2.3-1	229	6.56	2651.2	20
2.4-1	210	7.87	2440.2	20
2.5-1	240	5.88	886.2	6.30
2.5-2	220	6.78	2663.5	20
2.6-1	234	5.90	2933.1	20
2.6-2	238	8.62	903.6	8.64

Note: *the first number indicates the embedment length (in cm); the remaining two numbers describe the cube number and the fibre number (Figure 2b). Results of the "top" fibres (denoted as fibre "3") are not included in the table.

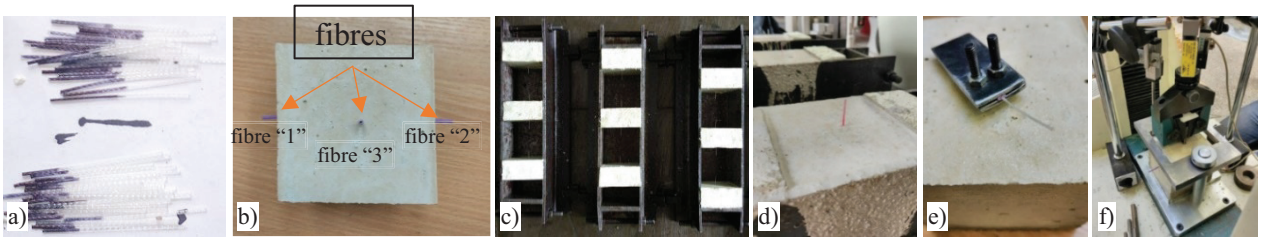

Figure 2. Test object: a) fibres highlighting the embedment length; b) a typical cube with embedded fibres; c) forms for production of the specimens; d) fibre protected with a plastic sleeve; e) steel clamps; f) testing machine

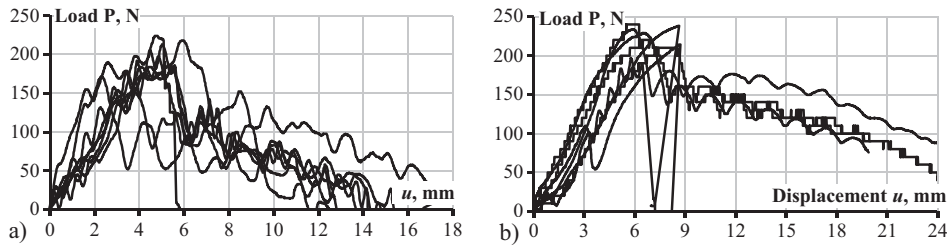

Figure 3. Load-displacement diagrams of the pull-out tests: a) embedment length l_e = 1 cm; b) l_e = 2 cm

of fibre (abnormal result); (III) bond damage before the test (abnormal result). The latter issue was mainly related with insufficient bond-strength of the "top" fibres. Sedimentation of fresh concrete could explain the reduction of mechanical properties of the bond (Gao et al., 2019). In all cases, bond characteristics of the fibres installed to the top surface of cubes were noticeably worse than the corresponding properties of the fibres positioned at the side surfaces, the pull-out forces required to pull out the "top" fibres were more scattered comparing with the "side" samples. Thus, further analysis is based only on the test outcomes of the "side" fibres. Figure 3 shows the corresponding load-displacement diagrams.

2. Numerical modelling

This section describes the development of the numerical model suitable to predict the deformation response of a synthetic macro-fibre. A commercial finite element (FE) software Atena (Červenka et al., 2018) is used for that purpose. The load-deformation diagrams shown in Figure 3 are the modelling object. The continuous pulling-out behaviour of the fibres is considered (i.e. failure of fibres was not modelled). Three stages of the deformation behaviour can be identified following the classification proposed in the referred work (Breitenbücher et al., 2014):

- Complete bonding – the adhesive contact ensure a perfect connection between the fibre surface and surrounding concrete.
- Failure of the bond starts when the pull-out force exceeds the adhesion shear resistance.
- Fibre slips due to the loss of the adhesive contact; the fibre sliding induces friction forces opposite to the pulling direction.

A strong chemical bond between the cement matrix and the fibre could form during the hardening process of the concrete (Signorini et al., 2020). It alters the mechanical properties of the concrete around the fibre. This narrow area is called the "transition zone". The reference (Bentur et al., 1985) limits the area of this zone to about 0.005 mm. This area is too small compared to the fibre diameter. That complicates the development of a detailed model of this zone. Thus, a simplified bond model describes the above process under the assumption of identical parameters of the concrete (independently on that it belongs to the transition zone or not). Still, there is no unified methodology to determine the parameters of the model (Wang et al., 1988). This study employs a trial-and-error approach to model bond behaviour. The model parameters were tailored to represent the test result of the embedment length of 1 cm (Figure 3a) adequately; the experimental outcomes of specimens having the 2 cm embedment length (Figure 3b) were used to verify the developed model.

The deformation problem is solved in the 3D formulation. Isoparametric tetrahedral elements with 10 degrees of freedom and four integration points are used. A rectangular shape replaced the round cross-section of the fibre simplifying the development of the FE model. The producer specified the 0.9 mm equivalent diameter of the fibre. The simplified geometry was calculated to represent the area and perimeter of the rectangle identical to the original dimensions. The 0.25×2.58 mm equivalent cross-section was obtained.

The 100 mm cube represented the concrete part of the specimen. The 10 mm and 150 mm global size of finite elements with 100 times refinement at the bond contact satisfying the mesh comparability condition were assumed for the fibre and concrete part, respectively. The resultant number of FE was approximately equal to 4000. Figure 4 shows the FE models of different embedment lengths.

The 3D Non-Linear Cementitious 2 User material model was assumed for the concrete. It is based on the concept of smeared cracks and damage (Zhang et al., 2019). Table 2 shows the model parameters of the concrete. The fibre was modelled as a perfectly elastic material. The elastic modulus = 3.35 GPa of and the Poisson ratio = 0.1 taken from the mill-certificate were assumed. These parameters were constant during the bond model adjusting procedure.

The prescribed deformations were applied to the free end of the fibre in a step-wise manner. The loading step = 0.25 mm was chosen. Thus, the simulations of 1 cm and 2 cm embedment lengths included 50 and 100 loading steps, correspondingly. The movements of the bottom surface of the specimen (Figure 4) were fixed in all directions. The solution procedure of the deformation problem

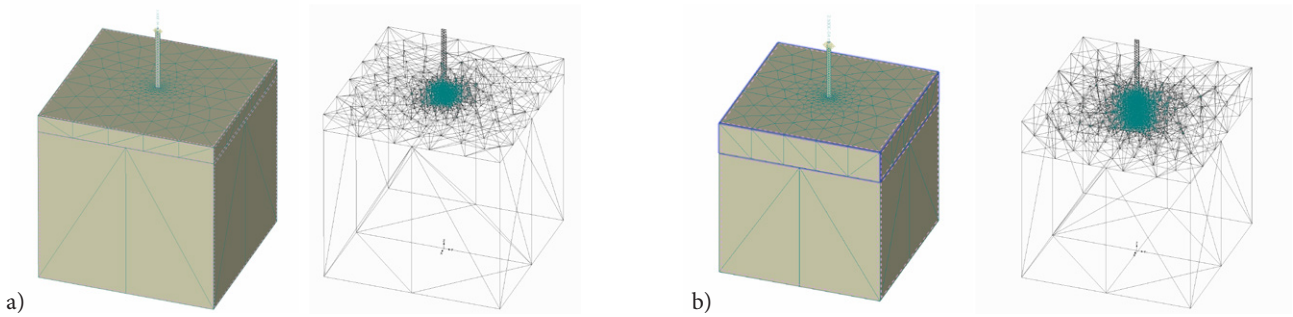

Figure 4. FE models of different bonding length: a) 1 cm and b) 2 cm embedded fibres

employed the Newton-Raphson iteration procedure assuming 40 iterations at each loading step.

The following parameters define the bond-model assumed in ATENA: the normal stiffness K_{nn}, the tangential stiffness K_{tt}, the tensile strength f_t, the cohesion factor C, and the friction coefficient μ. These parameters were tailored to represent adequately the load-deformation diagrams shown in Figure 3a. Figure 5a shows several initial solutions. The simulations were carried out until the prediction error does not exceed 5%. The average deformation energy δ of the fibre samples 1.1-1, 1.1-2, 1.3-1, 1.4-1, and 1.4-2 (Table 1) were used to estimate the prediction error. Figure 5b demonstrates the resultant prediction. Table 3 lists the accepted parameters of the bond model.

The pull-out test results of the fibres having 2 cm embedment length (Figure 3b) were used to verify the adequacy of the identified parameters of the bond model (Table 2). Figure 6 compares the simulation results of the test specimens with 1 cm and 2 cm bonding lengths. The predicted distributions of the shear stresses correspond to the loading points indicated at the load-displacement diagrams by the red dots.

The load-displacement diagrams presented in Figure 6 demonstrate adequate prediction results of both bonding lengths. The simulated and averaged experimental deformation energies of the 1 cm bonding length were correspondingly equal to 1118.3 Nmm and 1077.4 Nmm. That corresponds to the 4% approximation error. The

Table 2. Parameters of the concrete and bond models

Concrete model		Bond model	
Elastic modulus E_c	33.8 [GPa]	Normal stiffness K_{nn}	1500 [GN/m^3]
Poisson ratio ν	0.2	Tangential stiffness K_{tt}	1500 [GN/m^3]
Compressive strength *fc*	33.3 [MPa]	Tensile strength f_t	15.0 [MPa]
Tensile strength f_t	2.77 [MPa]	Cohesion factor C	7.0 [MPa]
Fracture energy G_f	6.92 [kN/m]	Friction coefficient μ	0.20 [–]

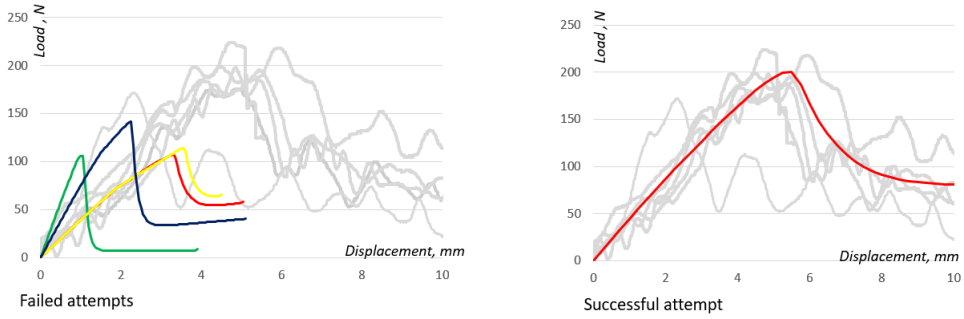

Figure 5. Load-displacement diagrams of the 1 cm bonding length: a) initial simulations; b) the resultant predictions using the bond parameters described in Table 2

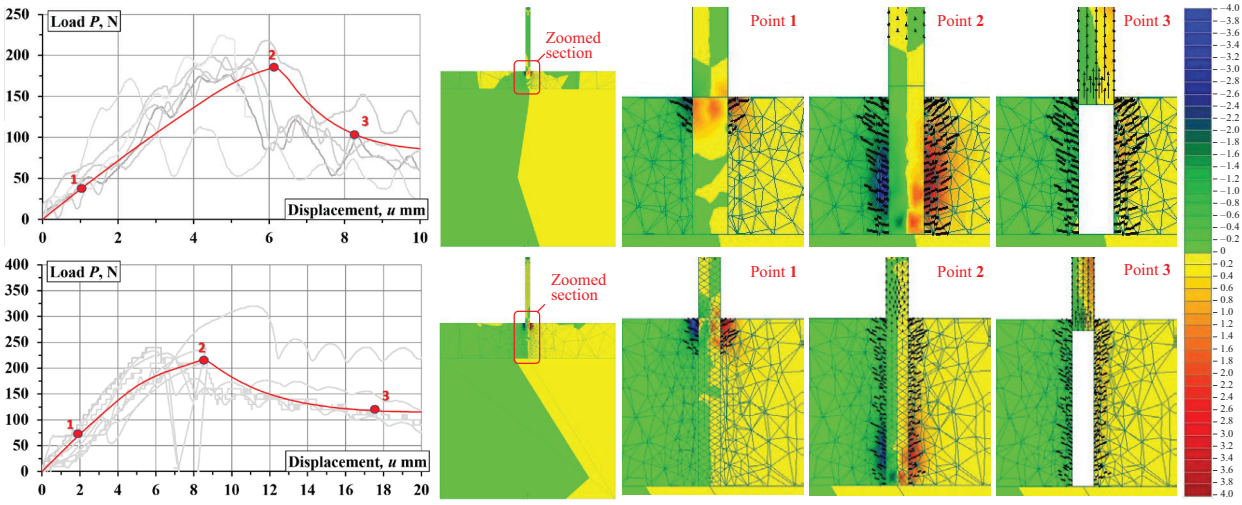

Figure 6. Simulation results (shear stresses) of different bonding lengths using the bond parameters described in Table 2: a) 1 cm length; b) 2 cm length

corresponding results of the 2 cm embedded fibre were approximated as 2746.3 Nmm and 2672.0 Nmm that determines the 3% error of the displacement prediction. The fibre samples 2.3-1, 2.4-1, 2.5-2, and 2.6-1 (Table 1) were used to determine the average energy δ. The results of 2 cm bonded fibre well agrees to the 1 cm fibre simulation outcome. That proves the adequacy of the developed bond model of the synthetic macro-fibre (Figure 2a).

The developed model is suitable to simulate the averaged deformation behaviour of synthetic fibres. A substantial scatter, however, is characteristic of the actual deformation behaviour of fibres (Figure 3). That makes the numerical predictions of particular fibres unreliable, but the mesoscopic models (e.g., Figure 1c) include numerous discrete fibres. Thus, the variations of the bond properties of the individual fibres become self-compensated (Bitencourt et al., 2019; Juhász, 2019).

Conclusions

This study investigates the bond behaviour of synthetic macro-fibres in concrete. A pull-out test of a single fibre is applied to investigate the mechanical performance of the bond. The corresponding load-displacement diagrams were analysed. Two bonding lengths (10 mm and 20 mm) were used. Eight cube specimens for each fibre length were produced. Three fibres (one on the top and two on the opposite sides) were inserted in each cube. Results of the "side" fibres were found suitable for the analysis. A physically non-linear finite element model of the pull-out sample was developed. A commercial software Atena was used to simulate the bond behaviour. The trial-and-error technique was used to set parameters of the bond model of the 1 cm embedment length. The 2 cm embedded fibres were used to verify the model. The identified bond model was found suitable to represent the deformation behaviour of synthetic macro-fibres. The prediction errors corresponding to the 1 cm and 2 cm simulation results do not exceed 4%. The developed model is suitable to simulate the averaged deformation behaviour of synthetic fibres characteristic of advanced mesoscopic models. Further research on nonlinear finite element simulation and analysis with a refined loading step size are recommended.

Author contributions

Mantas Garnevičius was responsible for data collection and analysis. Together with Linas Plioplys, he wrote the first draft of the article. Linas Plioplys was responsible for data interpretation and numerical modelling. Viktor Gribniak conceived the study and was responsible for the design and development of the data analysis. He also made the final proofread.

Disclosure statement

Authors declare that they have not any competing financial, professional, or personal interests from other parties.

References

Alberti, M. G., Enfedaque, A., Gálvez, J. C., & Ferreras, A. (2016). Pull-out behaviour and interface critical parameters of polyolefin fibres embedded in mortar and self-compacting concrete matrixes. *Construction and Building Materials*, *112*, 607–622. https://doi.org/10.1016/j.conbuildmat.2016.02.128

Babafemi, A. J., & Boshoff, W. P. (2017). Pull-out response of macro synthetic fibre from concrete matrix: Effect of loading rate and embedment length. *Construction and Building Materials*, *135*, 590–599. https://doi.org/10.1016/j.conbuildmat.2016.12.160

Bentur, A., Diamond, S., & Mindess, S. (1985). The microstructure of the steel fibre-cement interface. *Journal of Materials Science*, *20*, 3610–3620. https://doi.org/10.1007/BF01113768

Bitencourt, L. A. G., Manzoli, O. L., Bittencourt, T. N., & Vecchio, F. J. (2019). Numerical modeling of steel fiber reinforced concrete with a discrete and explicit representation of steel fibers. *International Journal of Solids and Structures*, *159*, 171–190. https://doi.org/10.1016/j.ijsolstr.2018.09.028

Breitenbücher, R., Meschke, G., Song, F., & Zhan, Y. (2014). Experimental, analytical and numerical analysis of the pullout behaviour of steel fibres considering different fibre types, inclinations and concrete strengths. *Structural Concrete*, *15*, 126–135. https://doi.org/10.1002/suco.201300058

Červenka, V., Jendele, L., & Červenka, J. (2018). *ATENA program documentation – part 1: theory*. Červenka Consulting.

Del Prete, C., Buratti, N., Manzi, S., & Mazzotti, C. (2019). Macro synthetic fibre reinforced concrete: Influence of the matrix mix design on interfacial bond behavior. *IOP Conference Series: Materials Science and Engineering*, *596*, 012025. https://doi.org/10.1088/1757-899X/596/1/012025

Gao, X., Zhang, J., & Su, Y. (2019). Influence of vibration-induced segregation on mechanical property and chloride ion permeability of concrete with variable rheological performance. *Construction and Building Materials*, *194*, 32–41. https://doi.org/10.1016/j.conbuildmat.2018.11.019

Juhász, K. P. (2019). The effect of the synthetic fibre reinforcement on the fracture energy of the concrete. *IOP Conference Series: Materials Science and Engineering*, *613*, 012037. https://doi.org/10.1088/1757-899X/613/1/012037

Oesch, T., Landis, E., & Kuchma, D. (2018). A methodology for quantifying the impact of casting procedure on anisotropy in fiber-reinforced concrete using X-ray CT. *Materials and Structures*, *51*, 73. https://doi.org/10.1617/s11527-018-1198-8

Signorini, C., Sola, A., Malchiodi, B., Nobili, A., & Gatto, A. (2020). Failure mechanism of silica coated polypropylene fibres for Fibre Reinforced Concrete (FRC). *Construction and Building Materials*, *236*, 117549. https://doi.org/10.1016/j.conbuildmat.2019.117549

Sivakumar, A., & Santhanam, M. (2007). A quantitative study on the plastic shrinkage cracking in high strength hybrid fibre reinforced concrete. *Cement & Concrete Composites*, *29*, 575–581. https://doi.org/10.1016/j.cemconcomp.2007.03.005

Vandewalle, L. (2000). RILEM TC 162 TDF: Test and design methods for steel fibre reinforced concrete. *Materials and Structures*, *33*, 3–5.

Wang, Y., Li, V. C., & Backer S. (1988). Modelling of fibre pull-out from a cement matrix. *International Journal of Cement Composites and Lightweight Concrete*, *10*, 143–149. https://doi.org/10.1016/0262-5075(88)90002-4

Zhang, J., Eisenträger, J., Duczek, S., & Song, C. (2019). Discrete modeling of fiber reinforced composites using the scaled boundary finite element method. *Composite Structures*, *235*, 111744. https://doi.org/10.1016/j.compstruct.2019.111744

BETONO IR SINTETINIO MAKROPLAUŠO SUKIBTIES SAVYBIŲ NUSTATYMAS IR MODELIAVIMAS

M. Garnevičius, L. Plioplys, V. Gribniak

Santrauka

Šio tyrimo objektas – sintetinio makroplaušo sukibties elgsena betone. Sukibties stiprumas ir standumas yra parametrai, apibūdinantys sukibties mechanizmą, kuris lemia armatūrinės medžiagos efektyvumą. Tačiau nėra bendros metodikos, kuria būtų galima įvertinti plaušo efektyvumą. Taip pat nėra nei paprasčiausios sintetinio makroplaušo sukibties kokybės įvertinimo procedūros, nei patikimo skaitmeninio modelio, kuris imituotų tokių plaušų sukibties elgesį. Šiame darbe 40 mm ilgio sintetinių makroplaušų sukibties mechanizmai tiriami atliekant ištraukimo bandymus. Tam buvo pagaminta 16 betono kubelių. Išbandoma viena iš rinkoje esančių sintetinių makroplaušų rūšių. Kiekviename bandinyje trys plaušai buvo įgilinami statmenai viršutiniam ir dviem šoniniams paviršiams. Buvo naudojami du įgilinimo ilgiai (10 mm ir 20 mm). Sukurta įtvirtinimo sistema, apsauganti plaušus nuo vietinių pažeidimų. Buvo sukurtas fiziškai netiesinis iš betono ištraukiamų plaušų baigtinių elementų modelis, pasiūlytas sukibties modelis, siekiant imituoti plaušų elgseną deformuojantis.

Reikšminiai žodžiai: sintetiniai plaušai, ištraukimas, bandymas, sukibties elgsena, skaitmeninis modeliavimas.